ELSEVIER

Optical Materials 16 (2001) 397–402

OPTICAL Materials
www.elsevier.nl/locate/optmat

Refractive indices of metastable and amorphous phases in Ne^{+}-ion irradiated magnesium–aluminate spinel

I.V. Afanasyev-Charkin [a,b], D.W. Cooke [a], M. Ishimaru [c], B.L. Bennett [a], V.T. Gritsyna [b], J.R. Williams [a,d], K.E. Sickafus [a,*]

[a] Materials Science and Technology Division, Los Alamos National Laboratory, MS-G755, Los Alamos, NM 87545, USA
[b] Department of Physics and Technology, Kharkiv National University, Svobody sq. 4, Kharkiv, 61077, Ukraine
[c] The Institute of Scientific Industrial Research, Osaka University, Minogaoka, Ibaraki, Osaka 567-0047, Japan
[d] Department of Materials Science and Engineering, University of Pittsburgh, Pittsburgh, PA 15213, USA

Received 3 February 2000; accepted 8 September 2000

Abstract

Single-crystal $MgAl_2O_4$ was subjected to 180 keV Ne^{+}-ion irradiation to fluences of (1, 5, and 10) $\times 10^{20}$ ions/m^2. The metastable and amorphous phases induced by irradiation were studied using transmission electron microscopy (TEM) and optical transmission spectroscopy. The thicknesses of implantation-induced layer structures were obtained from TEM observations. This information was then used in conjunction with optical transmission results to deduce the refractive indices of individual structures. It was found that the lowest ion fluence produces a metastable layer with a reduced index of refraction ($n = 1.70 \pm 0.005$) relative to the pristine substrate ($n = 1.72$), whereas the intermediate fluence induces an amorphous region ($n = 1.61 \pm 0.01$) bounded by metastable regions. The effect of the highest fluence is to increase the thickness of the amorphous layer ($n = 1.60 \pm 0.01$) at the expense of the metastable regions.

PACS: 78.20.Ci; 61.80.Jh; 61.16.Bg

Keywords: Spinel; Index of refraction; Ion implantation; TEM; Optical transmission

1. Introduction

Ion-beam implantation is an excellent technique for modifying the optical properties of materials. It typically produces a buried layer within the specimen, which is characterized by a reduced index of refraction relative to the pristine substance. This combination of high-index material bounded by a low-index layer produces an optical waveguide structure that can be tailored for various applications [1]. The profile of the buried layer and its index of refraction depend, among other things, on the type, energy, and fluence of ions used for implantation. Some materials require very high ion fluences to produce significant changes in the microstructure of the implanted region. An example of such a material is the oxide spinel.

Owing to its excellent radiation resistance, magnesium–aluminate spinel, $MgAl_2O_4$, has received considerable attention as a ceramic for use in high-radiation environments. Recent studies

* Corresponding author. Tel.: +1-505-665-3457; fax: +1-505-667-6802.
E-mail address: kurt@lanl.gov (K.E. Sickafus).

0925-3467/01/$ - see front matter
PII: S0925-3467(00)00048-3

have examined the radiation response of spinel at very high ion doses (e.g., [2]). Under cryogenic irradiation conditions (100 K), the principal findings were that amorphization occurred at a peak damage level of 25 displacements per atom (dpa) when single-crystal $MgAl_2O_4$ was irradiated with 400 keV Xe^{2+} ions. Moreover, prior to amorphization, $MgAl_2O_4$ transformed into a metastable phase characterized by a cubic unit cell with a smaller repeat length (4 nm) than that of undamaged spinel (8 nm).

In the present work, we irradiated $MgAl_2O_4$ with 180 keV Ne^+-ions at 100 K and measured, at room temperature, optical transmission for three different ion fluences. Recent experiments revealed that distinct metastable and amorphous regions are formed by Ne ion irradiation [3]. These were identified based on transmission electron microscopy (TEM) observations. In the study presented here, optical transmission data were obtained from these samples. The measurements revealed uniformly spaced oscillations as a function of wavelength. These are due to multiple interference of the light reflected at the various sample interfaces, each characterized by a different index of refraction. In this paper, we demonstrate that by combining TEM and optical transmission data, we are able to determine the refractive indices of the metastable and amorphous phases of $MgAl_2O_4$.

2. Experimental procedure

Single-crystals of $MgAl_2O_4$, obtained from the Linde Division of Union Carbide Corporation, were fabricated into samples appropriate for optical and TEM studies. Samples were 0.5 mm thick and were polished on both sides to an optical finish for use in the optical transmission studies.

Ion-beam irradiations were performed in the Ion Beam Materials Laboratory at Los Alamos National Laboratory using a 200 kV ion accelerator. Ne^+-ions of 180 keV energy were implanted into samples held at 100 K, which, following irradiation, were warmed to room temperature for optical and TEM studies. Samples were exposed to Ne^+-ion fluences (1, 5, and 10) $\times 10^{20}$ ions/m^2 at constant flux $(8.5 \pm 1) \times 10^{16}$ ions/m^2 s. To minimize ion-channeling effects during exposure, samples were tilted $\sim 7^\circ$ relative to the incident beam direction.

Ne^+-ion induced microstructure changes were examined using a JEOL JEM-3000F transmission electron microscope operating at 300 kV. Cross-sectional TEM samples were prepared using a combination of mechanical polishing and ion-thinning procedures, the latter with 4 keV Ar^+ ions.

Optical transmission measurements were carried out at room temperature on all samples before and after irradiation using a Cary 5E spectrophotometer operating in the wavelength regime 190–1000 nm (6.53–1.24 eV).

Calculations of ion range and energy deposition were made using the Monte-Carlo code SRIM-2000 (version 2000.10) by J.F.Ziegler et al. [4]. For the calculations, a density of 3.58 g cm^{-3} was used for stoichiometric spinel (JCPDS file 21-1152 [5]). A threshold displacement energy of 40 eV was used for all target elements (this choice is arbitrary). The results of SRIM calculations are shown in Fig. 1. The projected range of 180 keV Ne ions was estimated to be ~ 250 nm. The peak concentration of Ne at the fluence of 1×10^{21} ions/m^2 was about 6 at.%. According to SRIM calculations the thickness of sputtered material is ~ 9 nm.

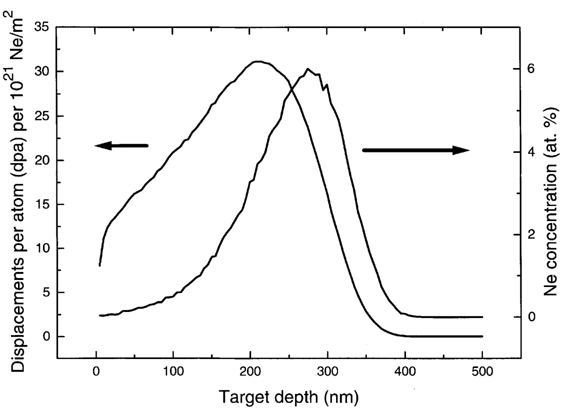

Fig. 1. Calculated number of atomic displacements produced by ions as a function of depth and range for 180 keV Ne ions in spinel based on SRIM Monte-Carlo simulations. A threshold displacement energy of 40 eV was used for all elements.

3. Results

Fig. 2 shows TEM bright-field images obtained from $MgAl_2O_4$ crystals irradiated with Ne^+ ions to fluences of (1, 5, and 10) $\times 10^{20}$ ions/m^2. The lowest Ne fluence induces a buried layer with a well-defined lower boundary adjacent to the irradiated substrate and a region of low damage at the surface. The structure of this buried layer was demonstrated (using electron diffraction) to be the metastable phase of spinel [3]. However, the intermediate Ne fluence (5×10^{20} ions/m^2) produces a buried amorphous layer [3], which is bounded by metastable phase layers [3], with the uppermost metastable layer extending nearly to the sample surface. At the highest Ne fluence, the thickness of the amorphous region increases while the surrounding metastable phase layers become thinner. The measured thicknesses of the various implantation layers is listed in Table 1.

Optical transmission spectra obtained from pristine unirradiated $MgAl_2O_4$ and from $MgAl_2O_4$ irradiated to a Ne^+ ion fluence of 1×10^{21} ions/m^2, are shown in Fig. 3. Transmission in the case of the irradiated sample exhibits oscillations at low energy ($E < 4.5$ eV). Also apparent in the radiation-induced transmission spectrum of Fig. 3 are the well-known absorption bands at 4.75 and

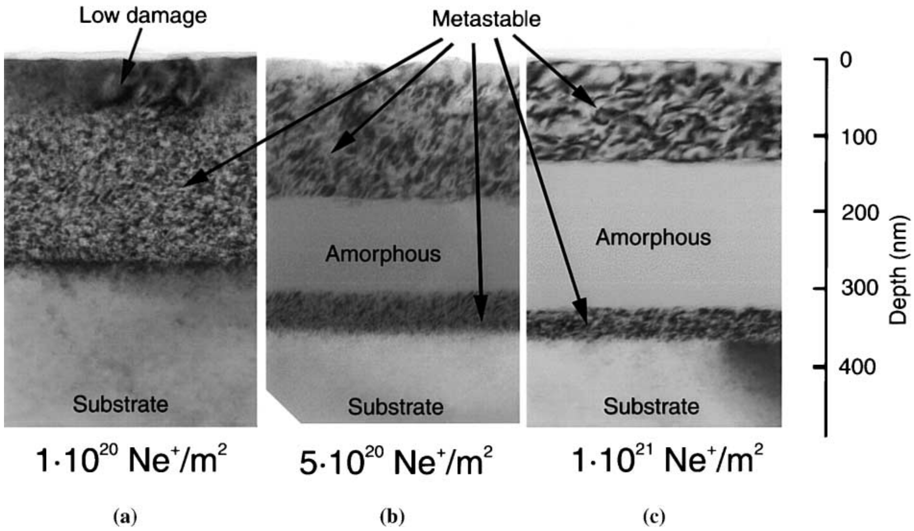

Fig. 2. TEM bright-field images obtained from $MgAl_2O_4$ irradiated with 180 keV Ne^+ ions to the following fluences: (a) 1×10^{20} ions/m^2; (b) 5×10^{20} ions/m^2; (c) 1×10^{21} ions/m^2 of 180 keV Ne^+-ions. Arrows indicate regions containing the metastable spinel phase. A depth scale is indicated on the right side of the figure.

Table 1
Thickness and refractive indices of the layered structures as a function of fluence

Fluence	Structure	Thickness (nm)	Refractive index
1×10^{20} ions/m^2	Undamaged	60	1.72
	Metastable	200	1.70 ± 0.005
5×10^{20} ions/m^2	Metastable	180	1.70 ± 0.005
	Amorphous	120	1.61 ± 0.01
	Metastable	45	1.70 ± 0.005
1×10^{21} ions/m^2	Metastable	135	1.70 ± 0.005
	Amorphous	190	1.60 ± 0.01
	Metastable	40	1.70 ± 0.005

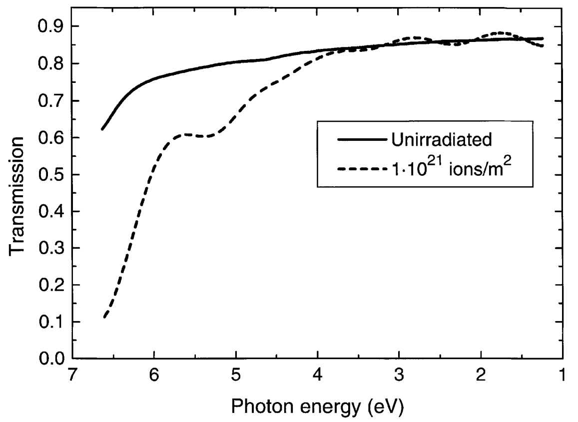

Fig. 3. Representative optical transmission spectra obtained from unirradiated (solid line) and Ne^{+}-ion irradiated (1×10^{21} ions/m^2) (dashed line) $MgAl_2O_4$ samples. Note the oscillations in the irradiated spectrum for $E > 4.5$ eV.

5.3 eV [6,7] (note that an absorption maximum corresponds to a transmission minimum). These radiation-induced absorption bands have been attributed to F^{+} centers (an electron trapped at an oxygen vacancy), and F centers (two electrons trapped at an oxygen ion vacancy), respectively [6,7]. Also after irradiation, an additional absorption band is induced near 6.9 eV. The maximum photon energy measured in our experiment was 6.53 eV; therefore, the position of this latter band was obtained by fitting the available experimental optical absorption data with a Gaussian band, which has been assigned to defect aggregates [8]. The optical transmission oscillations shown in Fig. 3 are due to multiple interference between light reflected at the various interfaces, each having a different index of refraction [1].

4. Analysis and discussion

TEM measurements of structural layer thicknesses (Table 1) and optical transmission spectral oscillation observations (Fig. 3) provide sufficient information to derive indices of refraction for the layers in the irradiated spinel material. Distinct optical oscillations occur in the spectral region where minimal optical absorption occurs, i.e., $E < 4.5$ eV. In this region of interest we can assume that $MgAl_2O_4$ is fully transparent, which is approximately correct according to Fig. 3. For simplicity, we further assume a constant index of refraction for pristine $MgAl_2O_4$ throughout the entire spectral region. The intensity of light transmitted through the irradiated sample can be written as

$$I = T_{\mathrm{irr}} \cdot I_0 = T_{\mathrm{d}} \cdot T_{\mathrm{s}} \cdot I_0, \tag{1}$$

where T_{irr} is the transmittance of an irradiated sample, T_{d} the transmittance of the damaged layer, T_{s} the transmittance of the undamaged substrate and I_0 is the intensity of the incident beam. Due to interference effects in the layers with altered indices of refraction, the transmittance T_{d} is different for different photon energies. The transmittance T_{s} is the same for all energies because the front and the back surfaces of the sample are not exactly parallel and, therefore, do not produce interference patterns. A multiple-layer film can be analyzed by representing each layer by a 2×2 matrix M_j [9], which has the form

$$M_j = \begin{pmatrix} \cos\delta_j & i\sin\delta_j/n_j \\ in_j\sin\delta_j & \cos\delta_j \end{pmatrix}, \tag{2}$$

where n_j is the refractive index of the layer and δ_j is a phase shift defined as

$$\delta_j = \frac{2\pi}{\lambda} n_j t_j \cos\theta_j, \tag{3}$$

where λ is the wavelength, t_j the thickness of layer j, and θ_j is the incidence angle of the light, which in the present experiment is equal to 0. The effect of a combination of N layers is obtained by taking a product of matrices representing each layer. Special matrices

$$\begin{pmatrix} n_0 & -1 \\ n_0 & +1 \end{pmatrix} \quad \text{and} \quad \begin{pmatrix} 1 \\ n_{\mathrm{s}} \end{pmatrix} \tag{4}$$

represent the top (air) and bottom (substrate) media with refractive indices of n_0 and n_{s}, respectively. The reflectivity of a thin-film multilayer is given by

$$R_{\mathrm{d}} = \left|\frac{a}{b}\right|^2, \tag{5}$$

where a and b are obtained from

$$\begin{pmatrix} a \\ b \end{pmatrix} = \begin{pmatrix} n_0 & -1 \\ n_0 & +1 \end{pmatrix} \times \prod_{j=1}^{N} \begin{pmatrix} \cos\delta_j & i\sin\delta_j/n_j \\ in_j\sin\delta_j & \cos\delta_j \end{pmatrix} \begin{pmatrix} 1 \\ n_s \end{pmatrix}. \quad (6)$$

Transmittance of the irradiated region of the sample in the absence of absorption is

$$T_d = 1 - R_d \quad (7)$$

and the transmittance of the unirradiated substrate can be obtained from the relation

$$T_s = \frac{4n_0 n_s}{(n_0 + n_s)^2}. \quad (8)$$

Transmittance of the unirradiated sample is given by

$$T_{unir} = \left(\frac{4n_0 n_s}{(n_0 + n_s)^2}\right)^2 = T_s^2. \quad (9)$$

In Fig. 3 we note that for the lowest measured energy (1.24 eV) $T_{unir} = 0.865$. Solving Eq. (9) we obtain $n_s = 1.72$, which is in reasonable agreement with the reported value for spinel ($n = 1.7123$ for $\lambda = 643.8$ nm, which corresponds to an energy of 1.93 eV) [10].

The effect of irradiation on sample transmittance can be determined by calculating the ratio of irradiated-to-unirradiated transmittance (using Eqs. (1) and (9)):

$$T = \frac{T_{irr}}{T_{unir}} = \frac{T_d \cdot T_s}{T_s^2} = \frac{1 - R_d}{T_s}. \quad (10)$$

Results of such calculations are shown in Fig. 4. For these calculations, layer thicknesses from TEM measurements were used, while the index of refraction of the irradiated layer was varied to obtain the best fit to the experimental data. Beginning with the low-fluence sample, which has only one altered layer, we determined the index of refraction of the metastable layer to be $n = 1.70$. The dashed line in the panel (a) of Fig 4 shows the theoretical curve that provides the best fit, which may be compared to the experimental transmission (solid line). The residual of these two curves is shown as a dotted line below. Using this value for the metastable phase, we proceed in a similar way to deduce n for the two variable thickness amorphous layers in the high-dose implanted spinel samples. The best fits are shown in Fig. 4 (panels (b) and (c)). Refractive indices of the 120 and 190 nm amorphous layers are found to be $n = 1.61$ and $n = 1.60$, respectively. Decrease in the refractive index of amorphous spinel for higher fluence may be caused by the increase in concentration of Ne in

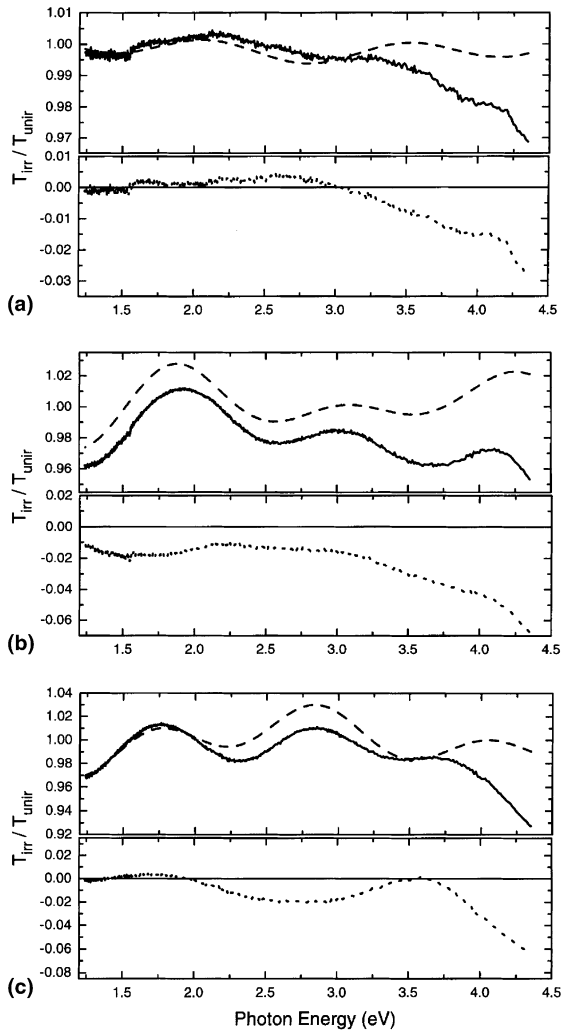

Fig. 4. Comparison of experimental and theoretical optical transmission spectra of $MgAl_2O_4$ exposed to various fluences of Ne^+-ions (a) 1×10^{20} ions/m^2; (b) 5×10^{20} ions/m^2; and (c) 1×10^{21} ions/m^2. In each panel the solid curve represents experimental results, the dashed curve represents theoretical results, and the dotted curve is a residual.

the implanted spinel crystal. According to SRIM simulations the peak concentration of Ne in spinel reaches 6 at.% at a fluence of 1×10^{21} ions/m^2.

It is difficult to place error bars on the extracted parameters because they derive from an iterative rather than statistical nonlinear least squares fitting routine. However, we examined the sensitivity of the best fit by varying n and observing concomitant changes in the residual curve. We found that variations in optimum n, which exceeded approximately 0.005 for the lowest dose and 0.01 for the higher doses, produced measurable changes. Therefore, we conclude that these values can be used as error estimates for our results.

A summary of the Ne^+-ion induced structures, thicknesses, and refractive indices for $MgAl_2O_4$ are given in Table 1. Low-fluence produces a metastable layer with a reduced index of refraction relative to the pristine substrate whereas the intermediate fluence induces an amorphous region with a further reduced index of refraction surrounded by metastable regions. The effect of the highest fluence is to increase the thickness of the amorphous layer at the expense of the metastable regions.

5. Conclusion

TEM measurements on single-crystal $MgAl_2O_4$ irradiated at 100 K with 180 keV Ne^+-ions, reveal the formation of layered structures that are fluence dependent. A metastable region of $\sim$200 nm thickness is formed when the sample is exposed to a fluence of 1×10^{20} ions/m^2, whereas an amorphous region ($\sim$190 nm thickness) bounded by metastable layers is induced when the fluence is increased five-fold. The structure of the layered regions remains unchanged upon a further two-fold increase in fluence, but the amorphous layer thickness increases at the expense of the metastable layer thickness.

Optical transmission data obtained from the irradiated specimens exhibit oscillations throughout the entire spectrum. This is attributed to multiple interference of the reflected beams at the various interfaces. Optical theory and knowledge of the layer thicknesses from TEM, were used to obtain a model fit to the experimental transmission data. This procedure yields the index of refraction for the layers in the irradiated samples. Using this procedure, we determined the refractive indices of the metastable and amorphous regions in $MgAl_2O_4$. The index of refraction of the metastable phase, $n = 1.70 \pm 0.05$, is slightly lower than the pristine substrate value of $n = 1.72$. In contrast, the two amorphous regions are characterized by thickness-dependent refractive indices with fitted values for the 120 and 190 nm thicknesses of $n = 1.61 \pm 0.01$ and 1.60 ± 0.01, respectively.

Acknowledgements

The authors acknowledge the assistance provided by Joseph Tesmer, Chris Wettland, Caleb Evans and Mark Hollander with ion implantations and Robert Dickerson for TEM assistance. This research was sponsored by the US Department of Energy, Office of Basic Energy Sciences, Division of Materials Sciences.

References

[1] P.D. Townsend, P.J. Chandler, L. Zhang, Optical Effects on Ion Implantation, Cambridge University Press, Cambridge, 1994.
[2] N. Yu, K.E. Sickafus, M. Nastasi, Philos. Mag. Lett. 70 (1994) 235.
[3] M. Ishimaru, I.V. Afanasyev-Charkin, K.E. Sickafus, Appl. Phys. Lett. 76 (2000) 2556.
[4] J.F. Ziegler, J.P. Biersak, U. Littmark, The Stopping and Range of Ions in Solids, Pergamon Press, New York, 1985.
[5] Powder Diffraction File, Joint Committee on Powder Diffraction Standards, Philadelphia, PA, 1974-present.
[6] G.S. White, K.H. Lee, J.H. Crawford, Appl. Phys. Lett. 35 (1979) 1.
[7] G.P. Summers, G.S. White, K.H. Lee, J.H. Crawford Jr., Phys. Rev. B 21 (1980) 2578.
[8] I.V. Afanasyev-Charkin, V.T. Gritsyna, D.W. Cooke, B.L. Bennett, C.R. Evans, M.G. Hollander, K.E. Sickafus, Nucl. Instr. Meth. B 148 (1999) 787.
[9] A. Nussbaum, R.A. Phillips, in: J.N. Holonyak (Ed.), Contemporary Optics for Scientists and Engineers, Prentice-Hall, Englewood Cliffs, 1976, p. 190.
[10] O. Medenbach, R.D. Shannon, J. Opt. Soc. Am. B 14 (1997) 3299.